Proc. XIX Int. Congr. Glass, Edinburgh, 1–6 July 2001 Phys. Chem. Glasses, 2002, **43C**, 38–47

Ultraviolet laser and x-ray induced valence changes and defect formation in europium and terbium doped glasses

H. Ebendorff-Heidepriem[1]

University of Southampton, Optoelectronics Research Centre, Southampton SO17 1BJ, UK

D. Ehrt

Friedrich Schiller University of Jena, Otto-Schott-Institut, Fraunhoferstr. 6, D-07743 Jena, Germany

The influence of Eu^{3+}, Eu^{2+} and Tb^{3+} ions on x-ray and ultraviolet laser induced defects is examined in a fluoride phosphate and an ultraphosphate glass. The defects are characterised by optical absorption, fluorescence and ESR spectroscopy. Europium ions cause larger changes in the fluoride phosphate glass whereas terbium ions do in the ultraphosphate glass. Different mechanisms of defect formation are found for x-ray and ultraviolet excimer laser irradiation at 248 nm. X-ray irradiation induces valence changes of a part of the dopant ions into $(Eu^{3+})^-$, $(Eu^{2+})^+$ and $(Tb^{3+})^+$ ions, respectively. By contrast, laser irradiation results in a very fast and complete photo-oxidation of Eu^{2+} but in a very slight photooxidation of Tb^{3+}. Photoreduction of Eu^{3+} does not occur. Under x-ray irradiation, the dopants have a similar but small influence on the intrinsic defect formation. Extrinsic rare earth related defect centres replace intrinsic defects. On the contrary, the laser induced photo-oxidation of Eu^{2+} enhances considerably the amount of intrinsic electron centres but suppresses effectively the formation of intrinsic hole centres. However, Tb^{3+} doping increases both electron and hole centre formation. These peculiarities of Eu^{2+} and Tb^{3+} doping result from the coincidence of the laser energy with the 4f–5d transitions of the rare earth ions. The fast and intense laser induced defect formation in the Eu^{2+} and Tb^{3+} doped glasses suggests that these dopants are promising candidates for increasing the photosensitivity of glasses.

Irradiation of glasses with sufficient high energy (x-ray, ultraviolet) releases electrons and holes which can be trapped by precursors in the matrix, leading to the formation of electron defect centres (EC) and hole defect centres (HC), absorbing in the ultraviolet and visible spectral region.[1] This results in undesired transmission losses of optical glasses.[1–7] Desired radiation induced effects are refractive index change and persistent spectral hole burning by ultraviolet laser irradiation as well as radiation stimulated fluorescence of active ions. These phenomena are used in photosensitive glasses, x-ray storage phosphors, scintillators and optical memory devices.[8–16]

Polyvalent rare earth ions such as europium and terbium can interfere in the releasing and trapping of electrons. Their valence state can be changed by high energy radiation such as x-ray and ultraviolet light.[15–29] Rare earth doping has an influence on radiation induced phenomena such as intrinsic defect centre formation,[17,20,30–2] laser induced refractive index modulation,[33–6] spectral hole burning[16,24–6,37] and radiation stimulated luminescence.[13–15,22,27–9,38] Thus fundamental research on rare earth doped glasses under irradiation is of importance to favour or suppress defect generation as required. Furthermore, polyvalent rare earth ions are suitable indicators for examination of the mechanisms of defect formation.

Under neutral melting conditions in air, europium and terbium ions occur predominantly in the trivalent state.[10,39] Eu^{3+} is an electron acceptor whereas Tb^{3+} is an electron donor. Thus the interactions between these ions and radiation induced defect formation are expected to be different for the individual ions. Using reducing melting conditions, Eu^{2+} ions can be formed in glasses.[20,22,26,38–42] They are electron donors like Tb^{3+} but they have considerably larger donor ability, i.e. oxidation tendency.[39]

Fluoride phosphate and phosphate glasses are attractive materials for high performance optics and for photonic devices.[2,6,43,44] Thus the study of radiation induced defect formation in these glasses is of special interest. The high ultraviolet transmission of the glasses enables the investigation of absorption and luminescence properties of metal ions and radiation induced defects. In addition the low viscosities and low melting temperatures make these glasses interesting model systems for examination of the redox behaviour of polyvalent ions.[45,46]

Recently we have examined systematically the impact of Eu^{3+}, Eu^{2+} and Tb^{3+} doping on the x-ray induced defect centre formation in fluoride phosphate and phos-

[1] Author to whom correspondence should be addressed. (e-mail: heh@orc.soton.ac.uk)

phate glasses. We found that the host glass composition has a large influence on the radiation induced redox behaviour of the rare earth ions.[31,32] In this paper, defect formation under ultraviolet laser irradiation is studied in addition to the two glasses showing the greatest difference: a fluoride phosphate glass (FP10) and an ultraphosphate glass (UP). The main focus of this paper consists of the comparison of both x-ray and ultraviolet laser induced valence changes of Eu^{3+}, Eu^{2+} and Tb^{3+}. Furthermore, the consequences of the interactions between high energy radiation and rare earth ions on the formation of intrinsic defect centres are of interest. Optical absorption, fluorescence and ESR spectroscopy have been used for identification and characterisation of the radiation induced defects and the redox states of the rare earth ions. Different mechanisms of defect formation have been found for x-ray and ultraviolet laser irradiation. From a practical point of view, the results on laser induced defect formation are promising for increasing the photosensitivity of glasses.

Experimental

The batch compositions of the two glass types studied were as follows (mol%).

FP10: 10 $Sr(PO_3)_2$.10MgF_2.30CaF_2.15 SrF_2.35AlF_3

UP: 3MgO.9BaO.10ZnO.9BaO.4Al_2O_3.65P_2O_5

High purity raw materials suitable for optical glasses were used. The FP10 glass samples were melted from fluorides and $Sr(PO_3)_2$. The UP glass samples were prepared from oxides and carbonates. The glasses were doped with europium and terbium ions using different raw materials: TbF_3 and EuF_3 for the FP10 glass, Eu_2O_3 and Tb_4O_7 for the UP glass. The Eu^{3+} and Tb^{3+} concentrations in the batches were 1×10^{19} ions cm^{-3} (730–890 ppmw Eu and 770–930 ppmw Tb, respectively).

At first the samples were melted from batches in air using platinum crucibles for the FP10 glass and silica glass crucibles for the UP glass. These samples are designated as FP10/air and UP/air, respectively. The rare earth ions in both glasses were found to occur solely in the trivalent state.[31,32,39] In order to generate Eu^{2+} ions, reducing melting conditions were employed. For FP10, the starting glasses were remelted in carbon crucibles in argon atmosphere at 1000°C in the case of the undoped glass and at 1100°C in the case of the doped glass (FP10/red). About 30% of the europium ions were found to be in the divalent state.[32,39] For UP, several methods were used: remelting the starting glasses in carbon crucibles in argon atmosphere, addition of sugar or aluminium powder to the batches and then melting the batches in silica glass crucibles in air. However, in no one sample could Eu^{2+} ions be detected.[32,39] The redox states and dopants of the samples used for irradiation experiments are listed in Table 1.

The glasses melted in platinum and silica crucibles were poured into graphite moulds and then slowly cooled to room temperature. The glasses melted in carbon crucibles were first rapidly cooled in the crucibles to about 800 K and then slowly cooled to room temperature. After annealing, the glasses were cut and polished into samples for irradiation and for measurement of the optical and ESR spectra. All glasses prepared are transparent and have an optical quality suitable for optical measurements.

Table 1. *Glass samples studied*

Glass	*Designation of redox state*	*Dopant under consideration*	*Rare earth concentration before irradiation relative to the whole doping of 1×10^{19} cm^{-3}*	
			Ln^{3+}	Eu^{2+}
FP10, UP	Air	None	–	–
		Eu^{3+}	100%	–
		Tb^{3+}	100%	–
FP10	Red	None	–	–
		Eu^{2+}	70%	30%

Glass samples of 0·5 mm thickness were irradiated with the unfiltered radiation of a Cu cathode x-ray tube working at 50 kV and 160 mA at room temperature. The distance between the samples and the x-ray tube was about 80 cm. The exposure duration time was about 20–30 h. Comparable conditions were obtained by simultaneous irradiation of samples. In the case of ultraviolet laser, glass samples of 2 or 4 mm thickness were irradiated using a KrF excimer laser at 248 nm (pulse energy 300 mJ/cm^2, repetition rate 5 Hz, pulse length 20 ns). For both x-ray and ultraviolet laser irradiation, the samples were irradiated several times at room temperature until saturation.

Absorption spectra in the range of 195–1000 nm were recorded at room temperature using a double beam spectrophotometer (Shimadzu UV-3101PC). The spectra shown were obtained by normalisation of the extinction (optical density), E, to the sample thickness, d (in cm). The radiation induced spectra were determined from spectra measured after and before irradiation. Band separations were carried out by least squares fitting using commercial computer software (Jandel Scientific Peakfit).

ESR measurements were carried out at X-band frequency (9·8 GHz) at room temperature using a commercial spectrometer (ESP 300E, Bruker). All spectra were recorded under the same conditions (accumulation, intensification). Therefore, different signal-to-noise ratios reflect different concentrations of the paramagnetic species which cause the ESR features.

Results

Europium and terbium ions cause intense ultraviolet absorption. Eu^{3+} ions show a broad charge transfer band at 200–210 nm whereas Eu^{2+} ions exhibit an intense and broad 4f–5d band peaked at 250 nm. Tb^{3+} ions demonstrate a comparatively sharp 4f–5d band at 210–215 nm, Figure 1.[39]

Eu^{2+} ions in FP10 glass exhibit several ESR signals in the range g=2–6. The most pronounced feature is located at g=6·0.[47]

X-ray irradiation of undoped and rare earth doped samples induces strong optical absorption in the visible and ultraviolet spectral region, Figure 2. Furthermore, intense ESR resonance lines are created in the range g=2–4 (290–400 mT at 9·8 GHz microwave frequency). Most of them are doublets indicating occurrence of hyperfine splitting due to neighbouring nuclei.[48–50]

Compared with the undoped samples, Eu^{3+} doping results in a more or less clear change of the x-ray in-

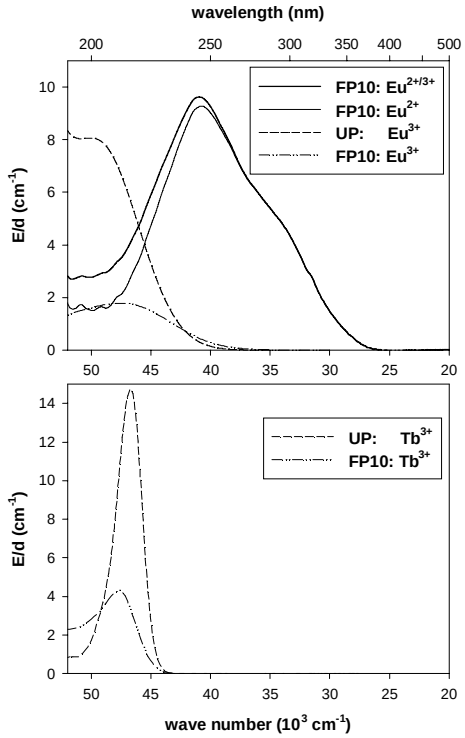

Figure 1. *Ultraviolet absorption spectra of europium and terbium ions in FP10/air and UP/air (Eu^{3+} and Tb^{3+}) as well as in FP10/red ($Eu^{2+/3+}$ and Eu^{2+}) glass samples. The spectra shown as bold lines for $Eu^{2+/3+}$, Eu^{2+} and Tb^{3+} were obtained by subtracting the spectra of the undoped samples from those of the rare earth doped samples (1×10^{19} ions cm^{-3}). The spectrum shown as a thin line demonstrates the absorption caused solely by Eu^{2+} ions*

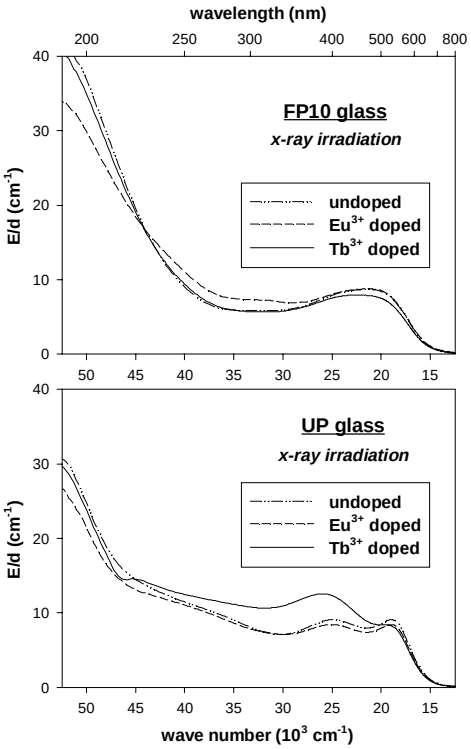

Figure 2. *X-ray induced absorption spectra measured immediately after irradiation of undoped, Eu^{3+} and Tb^{3+} doped FP10/air and UP/air glass samples*

duced absorption in the visible region. A uniform trend for all the glasses studied is not found.[32] However, the ultraviolet absorption clearly decreases due to Eu^{3+} doping, Figure 2. On the contrary, the presence of Eu^{2+} ions in FP10/red glass results in a considerable decrease of the radiation induced visible absorption, whereas the ultraviolet absorption remains constant, Figure 3. The doping with Tb^{3+} ions decreases the x-ray induced absorption in the high wavelength region (>520 nm) in both FP10 and UP glasses, whereas the ultraviolet absorption intensity remains nearly constant. Furthermore, the Tb^{3+} doped samples exhibit an additional absorption at 300–500 nm, Figure 2.

The effects on x-ray induced absorption caused by europium and terbium ions could be separated by normalisation of the spectra of the undoped samples to the intensity of the doped samples at about 500 nm as described in Ref. 31. As a consequence of the normalisation, the difference spectra between the induced absorption of the rare earth (Ln^{z+}) doped samples and the normalised absorption of the undoped samples (ΔLn^{z+} spectra) show the same absorption behaviour at higher wavelengths >450 nm. In the ΔEu^{3+} spectra, Figure 4, positive absorption at 230–400 nm and negative absorption <230 nm is observed. In the ΔEu^{2+} spectra of FP10/red samples, Figure 5(a), an opposite behaviour is found: negative absorption at 230–300 nm and positive absorption <230 nm. Similar to ΔEu^{3+} spectra, positive absorption occurs at 300–400 nm. In ΔTb^{3+} spectra, Figure 6, a broad band at about 370 nm and some ultraviolet absorption are observed. Furthermore, a steep decrease of the absorption intensity in the range of the pronounced Tb^{3+} absorption at 210–215 nm is found.

The compositional behaviour of the absorption intensity of the ΔLn^{z+} spectra differs for the individual rare earth ions. In the ΔEu^{3+} spectra, the FP10 glass demonstrates a clearly higher intensity than the UP glass, Figure 4. By contrast, in the ΔTb^{3+} spectra, the UP glass exhibits a considerably higher intensity, Figure 6.

Eu^{3+} ions hardly affect the intensity of the ESR lines of the intrinsic defect centres with respect to each other. By contrast, in the Eu^{2+} containing FP10/red sample, the doublet with signals at 310 and 380 mT demonstrates enhanced intensity with respect to the signal of the so called POHC (see section 4) at 346 mT, Figure

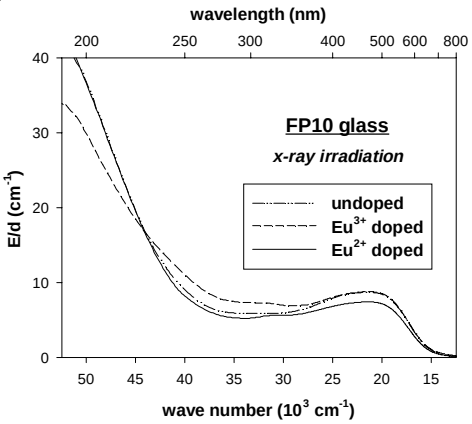

Figure 3. *X-ray induced absorption spectra measured immediately after irradiation of undoped and Eu^{3+} doped FP10/air and Eu^{2+} doped FP10/red glass samples*

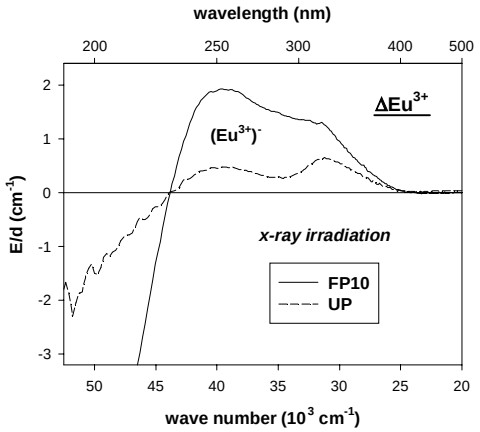

Figure 4. *ΔEu^{3+} spectra measured immediately after x-ray irradiation of FP10/air and UP/air glass samples*

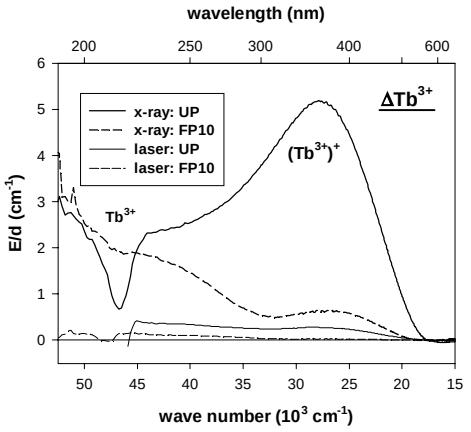

Figure 6. *ΔTb^{3+} spectra measured immediately after x-ray and laser irradiation, respectively, of FP10/air and UP/air glass samples*

7(a). Compared with the undoped samples, the Eu^{3+} doped samples exhibit additional ESR lines after x-ray irradiation. These lines are similar to Eu^{2+} ESR features. The occurrence of the g=6 signal in both the Eu^{2+} containing and the irradiated Eu^{3+} doped FP10 glass samples is especially evident, Figure 7(a). The ESR spectra of Tb^{3+} doped samples after x-ray irradiation exhibit an additional signal at 140 mT (g=5·0) compared with undoped samples, Figure 7(b). Furthermore, the intensities of the intrinsic defect centres are changed with respect to each other.

Laser irradiation results in absorption spectra of similar shape compared with x-ray irradiation. However, the laser induced absorption intensity is clearly lower, Figures 2, 8(a) and 9.

The Eu^{2+} doping has a very strong impact on the laser induced absorption of FP10/red glass. Already after 100 pulses irradiation, the characteristic Eu^{2+} absorption vanished and instead a very intense ultraviolet absorption is created, Figure 8(b). Further irradiation up to 2500 pulses until saturation does not cause pronounced modifications in the induced absorption spectrum. The absorption intensity in the visible region increases very slightly. The strong ultraviolet absorption changes their shape: The absorption intensity in the range 200–300 nm decreases whereas the one <200 nm increases, Figure 8(b). In contrast to the Eu^{2+} doping, 100 pulses laser irradiation of the undoped FP10/red sam-

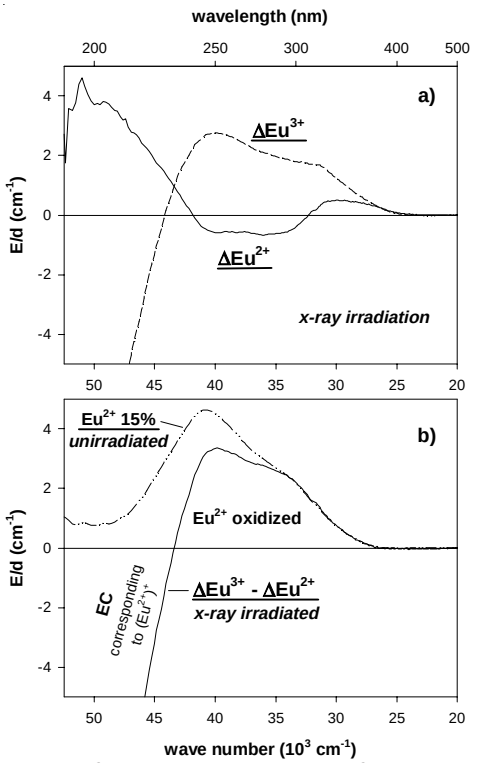

Figure 5. *(a) ΔEu^{3+} spectra of FP10/air and ΔEu^{2+} spectra of FP10/red samples as well as (b) the difference between the ΔEu^{3+} and ΔEu^{2+} spectra measured immediately after x-ray irradiation. Furthermore the absorption spectrum of Eu^{2+} ions in unirradiated FP10/red glass is shown*

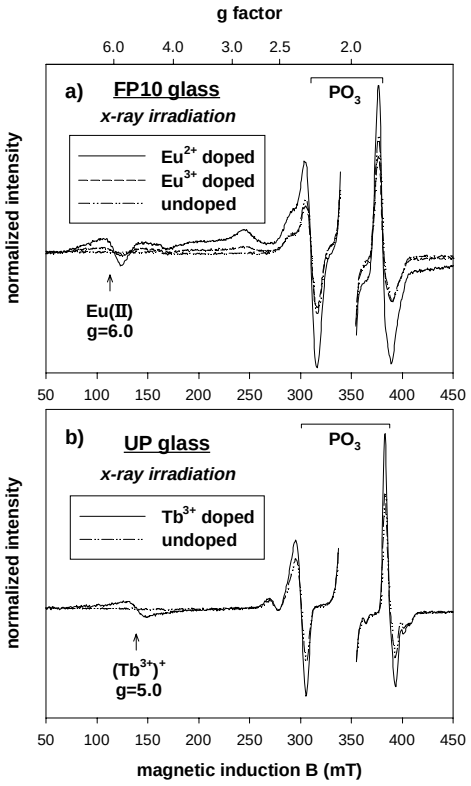

Figure 7. *ESR spectra normalised to the intensity of the POHC signal at 346 mT (g=2·021) of x-ray irradiated glass samples: (a) FP10/air:undoped, FP10/air:Eu^{3+} and FP10/red:Eu^{2+}; (b) UP/air:undoped, UP/air:Tb^{3+}. The spectra were measured after annealing at room temperature for 40–60 days*

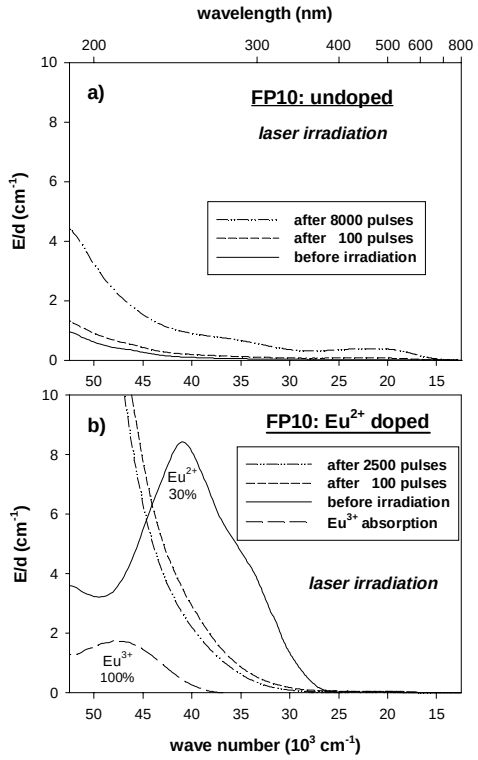

Figure 8. *Absorption spectra of (a) undoped and (b) Eu^{2+} doped FP10/red glass samples before and after laser irradiation. Furthermore, the absorption spectrum of 100% Eu^{3+} ions relative to the whole europium doping is shown*

ple results only in a very small induced absorption, Figure 8(a). At saturation after 8000 pulses laser irradiation, induced absorption is clearly observed in the visible and ultraviolet region. Compared with the Eu^{2+} doped sample, the visible absorption is clearly higher whereas the ultraviolet absorption is clearly lower, Figure 8(a).

ESR spectra confirm the strong impact of Eu^{2+} doping on laser induced defect formation. In the Eu^{2+} doped sample after laser irradiation until saturation, the doublet at 346 and 350 mT almost vanished whereas this doublet is clearly observed in the undoped sample. On the other side, the doublet at 310 and 380 mT has a clearly higher signal-to-noise ratio and thus higher intensity in the Eu^{2+} doped sample than in the undoped sample, Figure 10.

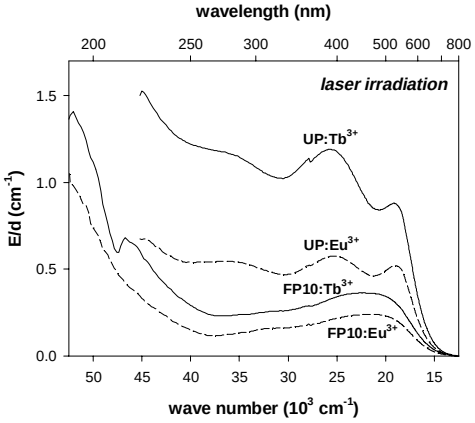

Figure 9. *Laser induced absorption spectra of Tb^{3+} and Eu^{3+} doped FP10/air and UP/air glass samples measured after saturation at about 9000–19000 pulses*

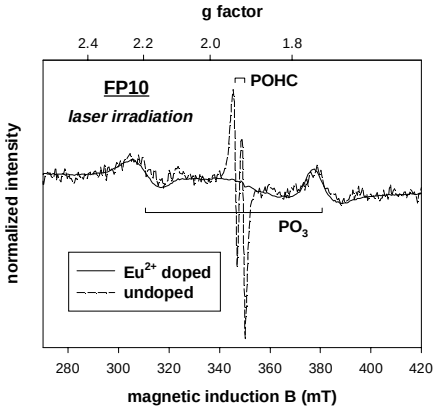

Figure 10. *ESR spectra normalised to the intensity of the PO_3 signal at 310 mT (g=2·256) of laser irradiated FP10/red glass samples measured after saturation (8000 pulses for the undoped and 2500 pulses for the Eu^{2+} doped sample)*

The laser induced absorption spectrum of the Eu^{3+} doped sample does not show differences in the shape compared with undoped FP10/air glass studied by Natura.[51] Furthermore, fluorescence spectra measured during laser irradiation showed solely the characteristic Eu^{3+} fluorescence at 590–790 nm; there was no indication of Eu(II) fluorescence.

Compared with Eu^{3+} doped samples, Tb^{3+} doping increases the laser induced absorption intensity from the visible to the ultraviolet region in both FP10 and UP samples. The Tb^{3+} doped UP sample demonstrates additionally a clearly higher absorption at 370 nm with respect to the absorption at 530 nm, Figure 9. Short-time irradiation of Tb^{3+} and undoped UP/air samples led also to a clearly higher induced absorption in the Tb^{3+} doped sample. Besides increasing the induced absorption intensity, Tb^{3+} doping enhances the rate of induced absorption generation, Figure 11.

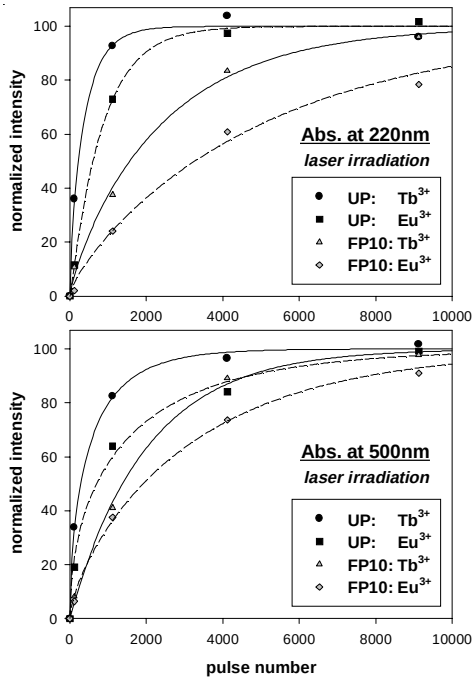

Figure 11. *Generation of laser induced absorptions at 220 and 500 nm which represent intrinsic EC and POHC, respectively, for Eu^{3+} and Tb^{3+} doped FP10/air and UP/air glass samples*

Discussion

Intrinsic defect formation

The absorption and ESR features as well as the structure of the intrinsic radiation induced defect centres in the glasses studied are assigned in accordance with Refs 48–50. The induced absorption in the visible region (290–600 nm) is mainly caused by holes trapped on phosphate groups, so-called phosphorus–oxygen hole centres (POHC). In the ultraviolet region (<290 nm), different electron centres localised on phosphorus atoms are found. They differ in the coordination number of surrounding oxygens: PO_4^-, PO_3^- and PO_2^-EC. The far ultraviolet absorption <200 nm results from defect centres of unknown structure. In the X-band ESR spectra, the intense doublet of low hyperfine splitting at 346 and 350 mT is attributed to POHC. The doublets of lower intensity but higher hyperfine splitting in the ranges of 270–330 mT and 360–400 mT are due to PO_4, PO_3 and PO_2 defect centres. The predominance of PO_3 among the PO_n^-EC is demonstrated by their high absorption and ESR intensity. The absorption and ESR features of the intrinsic HC and EC are summarised in Table 3 of Ref. 31.

Impact of rare earth ion doping on defect formation

By normalisation of the radiation induced absorption spectra of undoped samples to those of the doped samples, the effect of the rare earth ion doping could be revealed. In the ΔLn^{z+} spectra, the absorption due to intrinsic POHC and corresponding intrinsic EC is removed.

The similarity between the positive absorption at 230–400 nm in the ΔEu^{3+} spectra and the Eu^{2+} 4f–5d absorption, Figures 1 and 4, indicates x-ray induced reduction of Eu^{3+} ions to $(Eu^{3+})^-$ ions. In addition, the occurrence of the characteristic ESR signal of divalent europium ions at g=6 in the x-ray irradiated Eu^{3+} doped samples confirms the formation of radiation induced $(Eu^{3+})^-$ ions, Figure 7(a).

Thorough comparison of the absorption spectra of $(Eu^{3+})^-$ and Eu^{2+} ions in FP10 and phosphate glasses shows that the two ions have different environments in the FP10 glass. The local structure of $(Eu^{3+})^-$ in FP10 resembles the one of $(Eu^{3+})^-$ and Eu^{2+} in phosphate glasses. A detailed explanation of this phenomenon is reported in Ref. 32.

$(Eu^{3+})^-$ represents an EC due to the trapped electron compared with Eu^{3+}. Therefore, the negative ultraviolet absorption in the ΔEu^{3+} spectra, Figures 4 and 5(a), is assigned to intrinsic EC which are replaced by the extrinsic $(Eu^{3+})^-$-EC with respect to the undoped glasses. The lower ultraviolet absorption in the x-ray induced spectra of Eu^{3+} doped glasses, Figure 2, emphasises that the amount of intrinsic EC is lower in the Eu^{3+} doped glasses than in the undoped ones. Because of the comparatively low extinction coefficient of the Eu^{3+} charge transfer band at 200–210 nm, the decreasing concentration of Eu^{3+} ions due to formation of $(Eu^{3+})^-$ ions is not visible beside the intense negative absorption of the intrinsic EC replaced.[39] In the ESR spectra, the intensity ratio of PO_3-EC to POHC does not change clearly from undoped to Eu^{3+} doped samples. Therefore, the pronounced negative absorption is not caused by PO_3-EC but by nonparamagnetic EC.

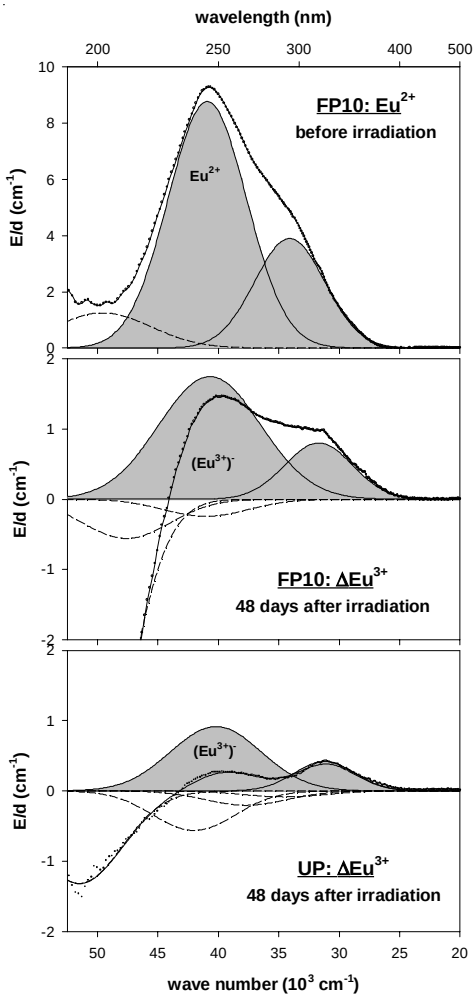

Figure 12. *Band separation of Eu^{2+} spectrum in FP10/red sample before irradiation and of ΔEu^{3+} spectra in x-ray irradiated FP10/air and UP/air samples measured after annealing at room temperature for 48 days*

The concentration of $(Eu^{3+})^-$ ions could be determined by means of band separation of the ΔEu^{3+} spectra using Gaussian bands as explained in detail in Ref. 32. For simulation of the $(Eu^{3+})^-$ absorption, two bands as for Eu^{2+} absorption are used, Figure 12. From the intensity of these two $(Eu^{3+})^-$ 4f–5d bands, the $(Eu^{3+})^-$ concentrations were calculated, Table 2.[32] Immediately, after x-ray irradiation, the amount of $(Eu^{3+})^-$ ions is clearly higher in the FP10 glass than in the UP glass. The same trend is found after annealing at room temperature for several weeks, because $(Eu^{3+})^-$ ions are destroyed in both glass types at nearly the same rate.[32] ESR spectra confirm the results of the absorption spectra. From the signal-to-noise ratio and from the intensity of the $(Eu^{3+})^-$ signal at g=6·0 with respect to a standard, a clearly higher $(Eu^{3+})^-$ concentration is also determined in the FP10 glass compared with the UP glass after annealing at room temperature for several weeks.[32]

The maximum Eu^{2+} absorption in FP10 glass is at 250 nm, Figure 1. Thus the negative absorption in the ΔEu^{2+} spectra around this wavelength, Figure 5(a), indicates decreasing Eu^{2+} amount. This reflects radiation induced oxidation to $(Eu^{2+})^+$ ions. The positive absorption

Table 2. *Influence of dopant and radiation source on the mechanisms of defect formation: amount of radiation induced ions immediately after irradiation with respect to the the ion concentration before irradiation, effect of doping on the intrinsic HC and EC amounts, short description of the radiation-induced defect formation caused by the dopants*

Radiation source	Dopant Ln^{z+} Radiation induced ion $(Ln^{z+})°$ Glass	Eu^{3+} $(Eu^{3+})^-$ FP10	UP	Eu^{2+} $(Eu^{2+})^+$ FP10	FP10	Tb^{3+} $(Tb^{3+})^+$ UP
X-ray	$(Ln^{z+})°/Ln^{z+}$ in %	4·2±0·4	2·7±0·3	50±5	5±1	10±1
	Effect on intrinsic EC amount	Decrease ↓		None		None
	Effect on intrinsic HC amount	None		Decrease ↓		Decrease ↓
	Mechanism	Substitution of intrinsic EC		Substitution of intrinsic HC		Substitution of intrinsic HC
Laser	$(Ln^{z+})°/Ln^{z+}$ (%)	0	0	100	0·5±0·1	<0·1
	Effect on intrinsic EC amount			Large increase ↑↑		Increase ↑
	Effect on intrinsic HC amount			Large decrease ↓↓		Increase ↑
	Mechanism			Fast & complete Photo-oxidation of Eu^{2+} Laser wavelength=4f–5d absorption		Energy transfer $Tb^{3+} \rightarrow PO_4$

>300 nm is attributed to $(Eu^{3+})^-$ absorption because of its similarity with the ΔEu^{3+} spectra in this region, Figure 5(a). The $(Eu^{3+})^-$ absorption could be eliminated from the ΔEu^{2+} spectra under the assumption that the number of the $(Eu^{3+})^-$ ions in the FP10/air and the FP10/red glass samples irradiated under the same conditions is similar. The ΔEu^{2+} spectra of FP10/red were subtracted from the ΔEu^{3+} spectra of FP10/air, Figure 5(b). The positive absorption of these difference spectra, 'ΔEu^{3+}–ΔEu^{2+}', designates the absorption of Eu^{2+} ions which are transformed to $(Eu^{2+})^+$ ions due to x-ray irradiation. The low energy tail of the Eu^{2+} absorption in the 'ΔEu^{3+}–ΔEu^{2+}' spectra equals the Eu^{2+} absorption in unirradiated FP10/red glass containing 15% Eu^{2+} ions relative to the whole europium doping, Figure 5(b) . This suggests that about half of the Eu^{2+} ions in the unirradiated samples has been oxidised by x-ray irradiation.

$(Eu^{2+})^+$ represents a HC due to the missing electron compared with Eu^{2+}. Therefore, the clear negative ultraviolet absorption in the 'ΔEu^{3+}–ΔEu^{2+}' spectra, Figure 5(b), is assigned to EC corresponding to the $(Eu^{2+})^+$-HC. The higher intensity of the ESR lines of PO_3-EC with respect to the ESR lines of POHC in the Eu^{2+} doped FP10/red glass compared to the undoped glass agrees with the clear negative ultraviolet absorption of PO_3-EC at 210 nm in the 'ΔEu^{3+}–ΔEu^{2+}'-spectra, Figures 5(b) and 7(a).

The lower POHC absorption intensity in the Eu^{2+} doped FP10 glass compared with the undoped and Eu^{3+} doped ones, Figure 3, indicates that the formation of $(Eu^{2+})^+$ ions suppresses the formation of POHC or that extrinsic $(Eu^{2+})^+$-HC are formed instead of intrinsic POHC.

In the ΔTb^{3+} spectra, Figure 6, the steep decrease of absorption intensity in the range of the pronounced Tb^{3+} band indicates a decrease of the Tb^{3+} concentration by the x-ray irradiation. Since Tb^{3+} is an electron donor, this result is attributed to radiation induced oxidation of Tb^{3+} ions to $(Tb^{3+})^+$ ions. Tetravalent terbium ions are expected to exhibit charge transfer bands because of their electron acceptor ability. Therefore, the broad band at 370 nm in the ΔTb^{3+} spectra is assigned to a charge transfer band of $(Tb^{3+})^+$ ions.[39] The pronounced ESR feature at g=5·0 is only observed in Tb^{3+} doped samples after x-ray irradiation. Thus this signal is attributed to radiation induced $(Tb^{3+})^+$ ions.[47]

$(Tb^{3+})^+$ represents a HC due to the missing electron compared with Tb^{3+}. Therefore, the ultraviolet absorption in the ΔTb^{3+} spectra, Figure 6, is assigned to EC corresponding to the $(Tb^{3+})^+$-HC. The higher intensity of the ESR lines of PO_3-EC with respect to the ones of POHC in the Tb^{3+} doped glasses compared to the undoped glasses agrees with the ultraviolet absorption of PO_3-EC at 210 nm in the ΔTb^{3+} spectra, Figures 6 and 7(b). This suggests that mainly PO_3-EC are formed in conjunction with the generation of $(Tb^{3+})^+$-HC.

The lower POHC absorption intensity in the Tb^{3+} doped glasses, Figure 2, indicates that the formation of $(Tb^{3+})^+$ ions suppresses the formation of POHC or that extrinsic $(Tb^{3+})^+$-HC are formed instead of intrinsic POHC.

The concentration of $(Tb^{3+})^+$ ions could be determined by band separation of the ΔTb^{3+} spectra using Gaussian bands, Figure 13.[31] From the intensity and extinction coefficient of the negative Tb^{3+} band, the concentration of Tb^{3+} ions which are transformed to $(Tb^{3+})^+$, i.e. the $(Tb^{3+})^+$ concentration, was calculated, Table 2. Since $(Tb^{3+})^+$ ions are stable at room temperature in both FP10 and UP,[31] the same compositional trend is found immediately after x-ray irradiation as well as after annealing at room temperature for several weeks. The amount of $(Tb^{3+})^+$ ions is clearly higher in the UP glass than in the FP10 glass. ESR spectra confirm this result. From the signal-to-noise ratio and from the intensity of the $(Tb^{3+})^+$ signal at g=5·0 with respect to a standard, a clearly higher $(Tb^{3+})^+$ concentration is also determined in the UP glass compared with the FP10 glass after annealing at room temperature for several weeks.[31]

Laser irradiation induces the same types of intrinsic defects like x-ray irradiation. However, because of the considerably lower energy of the laser radiation, the intensity of the defects is an order of magnitude lower, Figures 2, 8(a) and 9.

The disappearance of the characteristic Eu^{2+} absorption at around 250 nm already after 100 pulses laser irradiation, Figure 8(b), indicates very fast and complete photo-oxidation of Eu^{2+} to $(Eu^{2+})^+$. The ultraviolet absorption simultaneously induced is caused by intrinsic defect centres. Because of its low extinction coefficient, the charge transfer band of 100% Eu^{3+} relative to the whole europium doping can only contribute to a small extent to the high ultraviolet absorption, Figure 8(b). Likewise the photo-oxidation of Fe^{2+} ions cannot explain the high ultraviolet absorption because 100 pulses laser irradiation results only to a slight formation of $(Fe^{2+})^+$ ions in the undoped sample as described

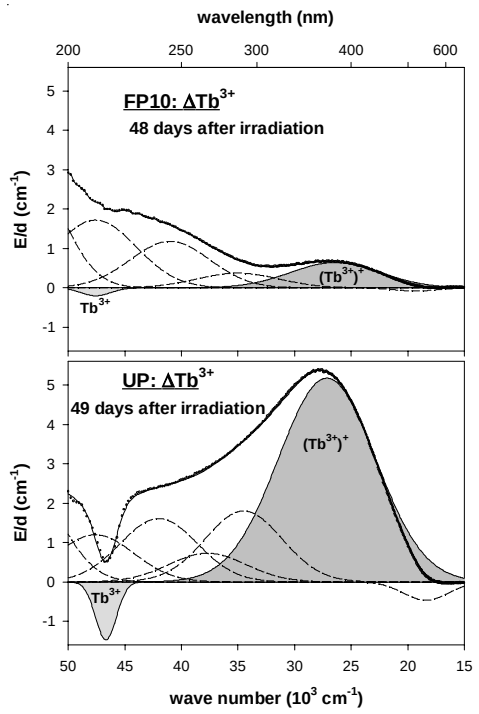

Figure 13. *Band separation of ΔTb^{3+} spectra of x-ray irradiated FP10/air and UP/air samples measured after annealing at room temperature for about 50 days*

below. Therefore, the ultraviolet absorption reflects intrinsic EC which are formed in conjunction with the generation of $(Eu^{2+})^+$-HC. The minute intensity in the high wavelength region of the $(Eu^{3+})^-$ absorption at 330–400 nm indicates that $(Eu^{3+})^-$ formation is unlikely. This result is consistent with the absence of Eu^{3+} reduction in Eu^{3+} doped glasses (see below).

Compared with the undoped FP10/red sample, the Eu^{2+} doping causes considerable differences in the defect formation. The very low POHC absorption in the Eu^{2+} doped sample, Figure 8(b), indicates that the photo-oxidation of the Eu^{2+} ions suppresses very effectively the POHC formation. The induced absorption at 260 nm in the undoped sample, Figure 8(a), results mainly from the absorption of $(Fe^{2+})^+$ ions formed under irradiation.[3–6] The formation of both POHC and $(Fe^{2+})^+$-HC in the undoped samples occurs gradually; saturation is achieved only after 8000 pulses. By contrast, the $(Eu^{2+})^+$-HC formation occurs very fast; it is already finished after 100 pulses. Further laser irradiation does not lead to a substantial POHC formation but to a transformation of the defect centres in the ultraviolet region. As a result, a slight decrease of the induced ultraviolet absorption >200 nm is observed. The ESR spectra of the undoped and Eu^{2+} doped FP10/red samples after laser irradiation until saturation confirm the results of the absorption spectra. The very low intensity of the POHC signals in the Eu^{2+} doped sample, Figure 10, agrees with the very low intensity of the POHC absorption in the visible region, Figure 8(b). The clearly higher signal-to-noise ratio of the PO_3 doublet at 310 and 380 mT in the Eu^{2+} doped sample indicates a considerably higher amount of PO_3 defect centres compared with the undoped sample. This suggests that PO_3 defect centres contribute to the EC formed together with the $(Eu^{2+})^+$-HC. It is worth mentioning that the same phenomenon was found in the case of x-ray irradiation.

In the Eu^{3+} doped FP10 and UP samples, fluorescence measurement during laser irradiation did not detect any formation of $(Eu^{3+})^-$ ions. In addition, absorption and ESR spectra do not yield any indication of $(Eu^{3+})^-$ formation. The shape of the laser induced absorption spectra of Eu^{3+} and undoped FP10 samples is identical. In the ESR spectra, no one characteristic Eu(II) signal is observed. Therefore, Eu^{3+} doping is assumed to have no substantial influence on the laser induced defect formation. On the contrary, the higher intensity of both intrinsic HC and EC absorption in the Tb^{3+} doped FP10 and UP samples after laser irradiation until saturation compared with the Eu^{3+} doped samples, Figure 9, suggests that Tb^{3+} doping intensifies both HC and EC formation. The short time laser irradiation of Tb^{3+} and undoped UP samples confirms this result. The additional induced absorption at 370 nm in the Tb^{3+} doped sample indicates formation of $(Tb^{3+})^+$ ions. In fact, the ΔTb^{3+} spectra reveals the broad $(Tb^{3+})^+$ absorption at 370 nm, Figure 6, and enables determination of the $(Tb^{3+})^+$ concentration, Table 2. ESR spectra of the laser irradiated samples demonstrate a higher intensity of the PO_3 signals relative to the POHC signals like the corresponding x-ray irradiated samples. This indicates formation of PO_3-EC for charge compensation of $(Tb^{3+})^+$-HC.

The generation of EC and POHC absorptions in dependence on laser pulse number, Figure 11, demonstrates that Tb^{3+} doping not only intensifies but also accelerates the intrinsic defect formation. Furthermore, the defect formation proceeds faster in the UP/air glass than in the FP/air glass which coincides with higher defect intensity in UP glass.

Comparison of x-ray and ultraviolet laser irradiation at 248 nm

The amount of radiation induced rare earth ions, $(Eu^{3+})^-$, $(Eu^{2+})^+$, $(Tb^{3+})^+$ and the influence of the rare earth doping on the defect formation is summarised in Table 2.

A small part of the Eu^{3+} ions (maximum 4% in FP10) is reduced by x-ray irradiation but not by laser irradiation. Because of its high energy much greater than the band gap between valence and conduction bands of the host glass, x-ray irradiation releases many electrons. As a result, even less effective or shallow electron traps like Eu^{3+} are filled. On the other side radiation induced oxidation of Eu^{2+} is less effective under x-ray irradiation than under laser irradiation. Thus the oxidation of $(Eu^{3+})^-$ during x-ray irradiation is less probable. Both electron avalanche and less effective oxidation of Eu(II) ions result in the presence of $(Eu^{3+})^-$ ions after x-ray irradiation.

Laser irradiation leads to a very fast and complete photo-oxidation of Eu^{2+} which prevents permanent photoreduction of Eu^{3+}. Under x-ray irradiation, only half of the Eu^{2+} ions are oxidised gradually.

X-ray irradiation induces a partial oxidation of Tb^{3+} ions (maximum 10% in UP), whereas the photo-oxida-

tion of Tb^{3+} under laser irradiation is very low (maximum 0·5% in UP).

The influence of rare earth doping on the defect formation under x-ray irradiation is similar for all three Ln^{z+} ions studied: substitution of intrinsic defect centres occurs. In the case of Eu^{2+} and Tb^{3+} doping, extrinsic $(Eu^{2+})^{+}$ and $(Tb^{3+})^{+}$-HC are formed instead of intrinsic POHC. Thus the amount of intrinsic EC remains nearly constant. By contrast, extrinsic $(Eu^{3+})^{-}$ ions replace intrinsic EC. It is worth noting that $(Eu^{2+})^{+}$ and $(Tb^{3+})^{+}$ ions are stable at room temperature in both FP10 and UP glasses, whereas $(Eu^{3+})^{-}$ ions are partly destroyed at room temperature.

Compared with x-ray irradiation, the laser induced defect formation at presence of Eu^{2+} and Tb^{3+} ions is different. In conjunction with the very fast and complete photo-oxidation of Eu^{2+}, intrinsic EC corresponding to the $(Eu^{2+})^{+}$-HC are formed and to a large extent also very fast. Thus the main part of the electron traps (precursors for EC) is already filled after 100 pulses laser irradiation. This prevents subsequent formation of intrinsic POHC and corresponding EC because most of the electrons released form the glass matrix by irradiation after $(Eu^{2+})^{+}$ formation cannot be trapped by unfilled precursors. Thus they react with holes or POHC resulting in nonformation or destruction of POHC. The reason for this mechanism of defect formation consists in the coincidence of the maximum of the Eu^{2+} 4f–5d energy at 250 nm, Figure 1, and the laser energy at 248 nm leading to effective excitation of the Eu^{2+} ions. This facilitates a complete removal of electrons resulting in $(Eu^{2+})^{+}$.

Considering the influence of the Tb^{3+} doping on laser induced defect formation, the increase of both HC and EC absorption intensity is remarkable. This suggests that Tb^{3+} doping sensitises the intrinsic HC and EC formation. The laser at 248 nm irradiates in the tail of the intense ^{7}F–^{7}D band at 210–215 nm, Figure 1, and/or in the maximum of the weak ^{7}F–^{9}D band at 250 nm[39] of the 4f–5d absorption. Subsequently, energy transfer from the excited state of Tb^{3+} ions to precursors in the glass matrix occurs leading to intensification and acceleration of the intrinsic defect formation. Similar sensitising effects are found for Pb^{2+} and Ce^{3+} in fluoride phosphate glasses[4,33,52,53] as well as for Tb^{3+} in aluminosilicate glass fibres.[34]

Eu^{2+} is completely photo-oxidised but Tb^{3+} is only very slightly oxidised by laser irradiation. This is due to different stability of the two valence states. The large stability of Eu^{3+} ions in glasses is the driving force for the photo-oxidation of Eu^{2+}. On the other side, the stability of Tb^{3+} ions makes their photo-oxidation less likely. Instead of that, the excited Tb^{3+} ions decay in the ground state by transferring its excess energy to precursors in the glass matrix. In general, sensitising ions such as Pb^{2+}, Ce^{3+} and Tb^{3+} are only partly oxidised by laser irradiation, so that enough ions remain for sensitisation of the intrinsic defect centre formation by energy transfer from the excited state of the lower valent ions.

The different mechanisms of x-ray and laser induced defect formation in the case of rare earth doping are summarised in Table 2.

The intense laser induced absorption in the Eu^{2+} and Tb^{3+} doped glasses is promising for increasing the photosensitivity of glasses. According to the colour centre model, photoinduced refractive index variations results from changes in the optical absorption spectrum especially in the ultraviolet region.[8]

Summary and conclusions

The influence of rare earth dopants on the defect formation is different for the two glass types studied. Europium ions cause larger changes in the FP10 glass whereas terbium ions do in the UP glass. The generation or transformation of divalent europium ions were determined by their characteristic properties: intense absorption at 250 nm, fluorescence at 400–450 nm and ESR features at g=6·0, 2·8, 2·0. The transformation of Tb^{3+} ions could be detected by the decrease of their intense and sharp absorption at 210 nm whereas the formation of tetravalent terbium ions was proven by their intense and broad absorption at 370 nm as well as the occurrence of their ESR feature at g=5·0.

In the Eu^{3+} doped FP10 glass, 4% of the doped ions are reduced to divalent $(Eu^{3+})^{-}$ ions by x-ray irradiation. The decrease of the EC absorption intensity in the ultraviolet suggests that the x-ray induced $(Eu^{3+})^{-}$ ions are formed instead of intrinsic EC. In contrast, photoreduction of Eu^{3+} could not be detected after laser irradiation in both glass types. In the Eu^{2+} doped FP10 glass sample, 50% of the Eu^{3+} ions are oxidised by x-ray irradiation. As a result, the intrinsic HC formation is suppressed as indicated by the decrease of the visible absorption. In contrast to x-ray irradiation, 100 pulses laser irradiation already induces a complete photooxidation of all the Eu^{2+} ions. The electrons released by this process form a high amount of EC absorbing in the ultraviolet. On the other side, the photo-oxidation suppresses effectively the intrinsic HC formation, since most of the EC precursors in the glass matrix are already filled by the electrons released from the Eu^{2+} ions. In the Tb^{3+} doped UP glass, nearly 10% of the Tb^{3+} ions are oxidised to tetravalent ions under x-ray irradiation, resulting in an additional absorption at 370 nm. In analogy to the Eu^{2+} doped FP10 glass sample, the x-ray induced oxidation of the Tb^{3+} ions suppresses slightly the intrinsic HC formation. Under laser irradiation, only 0·5% of the Tb^{3+} ions were photo-oxidised in the UP glass. The Tb^{3+} doping increases both HC and EC intensities compared with the Eu^{3+} doped samples in which the dopant did not interact with the laser irradiation. In addition, the rate of defect generation is enhanced. These results are attributed to energy transfer from the excited 5d configuration of Tb^{3+} to precursors in the glass matrix, supporting the formation of intrinsic defect centres.

The conspicuous effects of Eu^{2+} and Tb^{3+} ions on the laser induced defect formation are caused by their electronic structure. The laser energy at 248 nm populates the excited 5d configuration. Subsequent processes such as photo-oxidation (Eu^{2+}) and energy transfer (Tb^{3+}) interfere in the defect formation. The glass type affects the laser induced defect formation, too. In the UP glass, higher intensity as well as higher rate of defect generation is observed.

The fast and intense laser induced defect formation in the Eu^{2+} and Tb^{3+} doped glasses suggests that these dopants are promising candidates for increasing the photosensitivity of glasses.

Acknowledgement

The work was funded by the Thüringer Ministerium für Wissenschaft, Forschung und Kunst and by the Deutsche Forschungsgemeinschaft, Germany. We wish to thank A. Rambach and M. Friedrich for their help with the ESR measurements. We are grateful to U. Natura from the University of Jena, Germany, for the implementation of the laser irradiations.

References

1. Ehrt, D. & Vogel, W. Radiation effects in glasses. *Nucl. Instrum. Meth. Phys. Res. B*, 1992, **65**, 1–8.
2. Ehrt. D. Structure and properties of fluoride phosphate glasses. *Proc. SPIE*, 1992, **1761**, 213–21.
3. Ehrt, D., Ebeling, P. & Natura, U. UV transmission and radiation-induced defects in phosphate and fluoride phosphate glasses. *J. Non-Cryst. Solids*, 2000, **263&264**, 240–50.
4. Natura, U. Kinetics of UV laser radiation defects in high performance glasses. *Nucl. Instr. Meth. Phys. Res. B*, 2000, **166–167**, 470–5.
5. Natura, U. & Ehrt, D. Generation and healing behavior of radiation-induced optical absorption in fluoride phosphate glasses: the dependence on UV radiation sources and temperature. *Nucl. Instr. Meth. Phys. Res B*, 2000, **174**, 143–50.
6. Zou, X. & Toratani, H. Radiation resistence of fluorophosphates glasses for high performance optical fiber in the ultraviolet region. *J. Appl. Phys*., 1997, **81**, 3354–62.
7. Hosono, H., Mizuguchi, M., Kawazoe, H., Ichimura, T., Watanabe, Y., Shinkuma, Y. & Okawa, T. ArF excimer laser irradiation effects in AlF_3 based fluoride glasses for vacuum ultraviolet optics. *J. Appl. Phys*., 1999, **85**, 3038–43.
8. Potter, B. G. & Simmons-Potter, K. Photosensitive point defects in optical glasses: science and applications. *Nucl. Instrum. Meth. Phys. Res. B*, 2000, **166–167**, 771–81.
9. Edgar, A., Spaeth, J.-M., Schweizer, S., Assmann, S., Newman, P. J. & MacFarlane, D. R. Photostimulated luminescence in a rare earth-doped fluorobromozirconate glass ceramic. *Appl. Phys. Lett.*, 1999, **75**, 2386–8.
10. Blasse, G. & Grabmeier, B. D. *Luminescent materials*. 1994. Springer-Verlag Berlin-Heidelberg-New York.
11. Shaukat, S. F., McKinley, K. J., Flower, P. S., Hobson, P. R. & Parker, J. M. Optical and physical characteristics of HBLAN fluoride glasses containing cerium. *J. Non-Cryst. Solids*, 1999, **244**, 197–204.
12. Hirao, K. Photonics glass for PHB holographic memory. *J. Non-Cryst. Solids*, 1996, **196**, 16–25.
13. Hirao, K., Qiu, J. & Shimizugawa, Y. Photostimulable luminescence glasses as a novel material for optical memory. *Jpn. J. Appl. Phys*., 1998, **37**, 2259–62.
14. Qiu, J., Miura, K., Inouye, H., Kondo, Y., Mitsuyu, T. & Hirao, K. Femtosecond laser-induced three-dimensional bright and long-lasting phosphorescence inside calcium aluminosilicate glasses doped with rare earth ions. *Appl. Phys. Lett*., 1998, **73**, 1763–5.
15. Qiu, J. External electromagnetic field induced electronic structures and novel optical functions of rare-earth-ion-doped glasses. *J. Ceram. Soc. Jpn*., 2001, **109**, S25–S31.
16. Fujita, K., Nishi, M., Tanaka, K. & Hirao, K. Room-temperatur photochemical hole burning of Eu^{3+} in sodium borate glasses. *J. Phys.: Condens. Matter*, 2001, **13**, 6411–19.
17. Arbuzov, V. I., Nikolaev, Yu. P. & Tolstoi, M. N. Mechanism of intrinsic and impurity color center formation in sodium silicate glasses with two activators. *Fiz. Khim. Stekla*, 1990, **16**, 25–32.
18. Arbuzov, V. I. & Elerts, M. A. Photostimulated electron transfer between rare-earth coactivators in alkali silicate glasses. *Sov. J. Glass Phys. Chem*., 1992, **1**, 216–23.
19. Arbuzov, V. I., Grabovskis, V. Y. & Dzenis, Y. Y. Peculiarities of excitation of Ce^{3+} and Tb^{3+} x-ray luminescence in silicate glasses. *Sov. J. Glass Phys. Chem*., 1992, **18**, 147–51.
20. Arbuzov, V. I. & Kovaleva, N. S. Radiation-induced reduction of Eu^{3+} ions and its influence on color centers formation in phosphate glass. *Fiz. Khim. Stekla*, 1994, **20**, 492–9.
21. Arbuzov, V. I. Photostimulated electron transfer between coactivator ions in alkali silicate glasses. *J. Non-Cryst. Solids*, 1999, **253**, 37–49.
22. Qiu, J., Shimizugawa, Y., Iwabuchi, Y. & Hirao, K. Photostimulated luminescence in Eu^{2+} doped fluoroaluminate glasses. *Appl. Phys. Lett*., 1997, **71**, 759–61.
23. Qiu, J., Kojima, K., Miura, K., Mitsuyu, T. & Hirao, K. Infrared femtosecond laser pulse-induced permanent reduction of Eu^{3+} to Eu^{2+} in a fluorozirconate glass. *Opt. Lett*., 1999, **24**, 786–8.
24. Fujita, K., Tanaka, K., Hirao, K. & Soga, N. High-temperature persistent spectral hole burning of Eu^{3+} ions in silicate glasses: new room-temperature hole-burning materials. *J. Opt. Soc. Am. B*, 1998, **15**, 2700–5.
25. Nogami, M. & Ito, S. Spectral hole burning and x-ray irradiation in Eu^{3+}-doped glass. *Phys. Rev. B*, 2000, **61**, 14295–8.
26. Chung, W. J. & Heo, J. Room temperatur persistent spectral hole burning in x-ray irradiated Eu^{3+}-doped borate glasses. *Appl. Phys. Lett*., 2001, **79**, 326–8.
27. Hosono, H., Kinoshita, T., Kawazoe, H., Yamazaki, M., Yamamoto, Y. & Sawanobori, N. Long lasting phosphorescence properties of Tb^{3+}-activated reduced calcium aluminate glasses. *J. Phys.: Condens. Matter*, 1998, **10**, 9541–7.
28. Kinoshita, T., Yamazaki, M., Kawazoe, H. & Hosono, H. Long lasting phosphorescence and photostimulated luminescence in Tb-ion-activated reduced calcium aluminate glasses. *J. Appl. Phys*., 1999, **86**, 3729–33.
29. Kinoshita, T. & Hosono, H. Materials design and example of long lasting phosphorescent glasses utilizing electron trapped center. *J. Non-Cryst. Solids*, 2000, **274**, 257–63.
30. Ebendorff-Heidepriem, H. & Ehrt, D. Rare earth ions as indicators for radiation-induced defect center formation in phosphate containing glasses. *Phosphorus Res. Bull*., 1999, **10**, 552–6.
31. Ebendorff-Heidepriem, H. & Ehrt, D. Effect of Tb^{3+} ions on x-ray induced defect formation in phosphate containing glasses. *Opt. Mater*. 2002, **18**, 419–30.
32. Ebendorff-Heidepriem, H. & Ehrt, D. Effect of europium ions on x-ray induced defect formation in phosphate containing glasses. *Opt. Mater*., 2002, **19**, 351–63.
33. Williams, G. M., Tsai, T.-E., Merzbacher, C. I. & Friebele, E. J. Photosensitivity of rare earth doped ZBLAN fluoride glasses. *J. Lightwave Technol*., 1997, **15**, 1357–62.
34. Taunay, T., Bernage, P., Martinelli, G., Douay, M., Niay, P., Bayon, J. F. & Poignant, H. Photosensitization of terbium doped alumino-silicate fibres through high pressure H_2 loading. *Opt. Commun*., 1997, 133, 454–62.
35. Xie, W. X., Bernage, P., Ramecourt, D., Douay, M., Taunay, T., Niay, P., Boulard, B., Gao, Y., Jacoboni, C., Da Costa, A., Poignant, H. & Monerie, M. UV induced permanent gratings in Ce^{3+} or Eu^{2+} doped PZG glass thin-film waveguides deposited on CaF_2 substrates. *Opt. Commun*., 1997, **134**, 36–42.
36. Hamad, A. Y., Wicksted, J. P. & Dixon, G. S. The effect of write-beam wavelength on the grating formation in Eu^{3+}-doped alkali silicate glasses. *Opt. Mater*., 1999, **12**, 41–5.
37. Beck, W., Karasik, A. Ya., Arvanitidis, J. & Ricard, D. Persistent spectral hole hole-burning in a Eu^{3+}-doped aluminosilicate glass from 8 to 295K: Study of the burning and refilling kinetics, and of optical dephasing. *Eur. Phys. J. D*, 2000, **10**, 131–40.
38. Qiu, J., Miura, K., Inouye, H., Fujiwara, S., Mitsuyu, T. & Hirao, K. Blue emission induced in Eu^{2+}-doped glasses by femtosecond laser. *J. Non-Cryst. Solids*, 1999, **244**, 185–8.
39. Ebendorff-Heidepriem, H. & Ehrt, D. Formation and UV absorption of cerium, europium and terbium ions in different valencies in glasses. *Opt. Mater*., 2000, **15**, 7–25.
40. Tanaka, K., Fujita, K., Matsuoka, N., Hirao, K. & Soga, N. Large Faraday effect and local structure of alkali silicate glasses containing divalent europium ions. *J. Mater. Res*., 1998, **13**, 1989–95.
41. MacFarlane, D. R., Newman, P. J., Cashion, J. D. & Edgar, A. *In situ* generation of Eu^{2+} in glass-forming melts. *J. Non-Cryst. Solids*, 1999, **256&257**, 53–8.
42. Kucuk, A. & Clare, A. G. Optical properties of cerium and europium doped fluoroaluminate glasses. *Opt. Mater*., 1999, **13**, 279–87.
43. Weber, M. J. Science abd technology of laser glass. *J. Non-Cryst. Solids*, 1990, **123**, 208–22.
44. Ehrt, D., Carl, M., Kittel, T., Müller, M. & Seeber, W. High performance glass for the deep ultraviolet range. *J. Non-Cryst. Solids*, 1994, **177**, 405–19.
45. Ehrt, D., Leister, M. &Matthai, A. Redox behaviour in glass forming melts. *Molten Salt Forum*, 1998, **5–6**, 547–54.
46. Ehrt, D. Redox behaviour of polyvalent ions in the ppm range. *J. Non-Cryst. Solids*, 1996, **196**, 304–8.
47. Ebendorff-Heidepriem, H. & Ehrt, D. Electron spin resonance spectra of Eu^{2+} and Tb^{4+} ions in glasses. *J. Phys.: Condens. Matter*, 1999, **11**, 7627–34.
48. Ebeling, P. Radiation defects in glasses - a correlation of optical und ESR spectra. *PhD Thesis*. 1999. Friedrich Schiller University of Jena, Germany.
49. Ebeling, P., Ehrt, D. & Friedrich, M. Study of radiation-induced defects in fluoride-phosphate glasses by means of optical and EPR spectroscopy. *Glastech. Ber. Glass Sci. Technol*., 2000, **73**, 156–62.
50. Ebeling, P., Ehrt, D. & Friedrich, M. X-ray induced effects in phosphate glasses. Submitted to *Opt. Mater*.
51. Natura, U. UV radiation induced defect formation and annealing in glasses. *PhD Thesis*. 1999. University of Jena, Germany.
52. Natura, U. & Ehrt, D. Modeling of excimer laser radiation induced defect generation in fluoride phosphate glasses. *Nucl. Instrum. Meth. Phys. Res. B*, 2000, **174**, 151–8.
53. Ebendorff-Heidepriem, H. & Ehrt, D. UV radiation effects in fluoride phosphate glasses. *J. Non-Cryst. Solids*, 1996, **196**, 113–17.